COMMUNICATION

Liquid-liquid interface-promoted formation of a luminescent porous molecular crystal built from a supramolecular platinum(II)-hexamer

Received 00th January 20xx,
Accepted 00th January 20xx

DOI: 10.1039/x0xx00000x

Mari Kimura,[a] Masaki Yoshida,*[a] Sho Fujii,[a] Atsushi Miura,[a] Kosei Ueno,[a] Yasuhiro Shigeta,[a,b] Atsushi Kobayashi [a] and Masako Kato *[a]

Porous molecular crystals (PMCs) should function as new-generation functional porous materials, but selective crystallisation of PMCs is still difficult. Herein we demonstrate that liquid-liquid interface promotes crystallisation of a Pt(II)-based PMC, rather than the nonporous form, when immiscible solvent pairs are used, thereby allowing the control of luminescence.

Porous materials comprising organic units constitute a rapidly developing field in the past few decades. In particular, porous molecular crystals (PMCs) have recently attracted increasing attention as a new generation of functional porous materials.[1] PMCs offer several advantages over other porous materials, such as metal-organic frameworks (MOFs)[2] and covalent organic frameworks (COFs).[3] Typical advantages of PMC-based adsorbents[4] are facile fabrication via solution processes and ease of recycling after use.[1] These are because PMCs are constructed with weak and diverse interactions, including hydrogen bonds, π-π interactions, halogen interactions, and metallophilic interactions between molecules. The flexibility resulting from the weak interactions is also an important feature of PMCs because it enables control of the physical properties[5] and porosity[6] of PMCs through the use of weak and gentle stimuli. In addition, the construction of PMCs by metal complexes further allows us to achieve cooperative phenomena resulting from the flexible porous structures and the functionality of the metal complexes, such as vapochromism, phosphorescence, and magnetism.[7,8] Thus, PMCs are promising candidates for adsorption materials and also for stimuli-responsive materials with high structural order.[9]

Conversely, because PMCs are supported by weak and diverse interactions, their diversity sometimes complicates the

[a] *Department of Chemistry, Faculty of Science, Hokkaido University, North-10 West-8, Kita-ku, Sapporo, Hokkaido 060-0810, Japan. E-mail: myoshida@sci.hokudai.ac.jp, mkato@sci.hokudai.ac.jp*

[b] *Current address: Nanomaterials Research Institute, Kanazawa University, Kakuma-machi, Kanazawa, Ishikawa 920-1192, Japan.*

† Electronic Supplementary Information (ESI) available: Experimental detail, X-ray crystallographic data, spectral data, microscopic images, and theoretical calculations. CCDC 2003915-2003918. See DOI: 10.1039/x0xx00000x

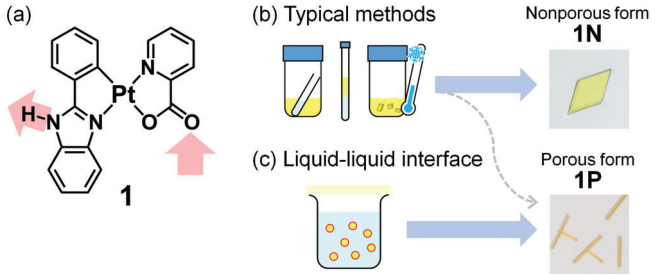

Scheme 1 (a) Structural formula of **1**. Pink arrows indicate the direction of the hydrogen-bond. (b, c) Schematic images of the crystallisation of **1N** and **1P** (b) by typical methods or (c) at liquid-liquid interface, respectively.

selective construction of porous structures.[1] Since porous crystals are intrinsically unstable compared to nonporous crystals, the crystallisation of PMCs requires more precise conditions than those required for MOFs or COFs. Even if the building block molecules are carefully designed, the formation of the desired PMCs still depends strongly on crystallisation conditions, such as solvent, temperature, and crystallisation time.[1f] Although several attempts have been made to solve this problem by using templates,[10] temperature-control was still required in some cases and the establishment of a selective crystallisation method remains a challenging issue for which improvements are required.

In this study, we have succeeded in the selective crystallisation of a new luminescent PMC consisting of the cyclometalated Pt(II) complex [Pt(pbim)(pic)] (**1** in Scheme 1(a); pbim = 2-phenylbenzimidazolate, pic = α-picolinate), which bears hydrogen-bond donor/acceptor sites. Although nonporous crystals (named as **1N**) were obtained preferentially with typical crystallisation methods (Scheme 1(b)), the desired PMC (named as **1P**) was selectively obtained at the interface formed between a MeOH/H_2O mixture and an alkane (Scheme 1(c)). Optical microscopic and microspectroscopic analyses suggest that the selective crystallisation of **1P** results from the stabilisation of porous channels composed of hydrogen-bonded cyclic hexamers of **1** at the liquid-liquid interface. Because of differences in crystal packing, the luminescent properties of **1** can also be successfully controlled with the use of **1P** and **1N**.

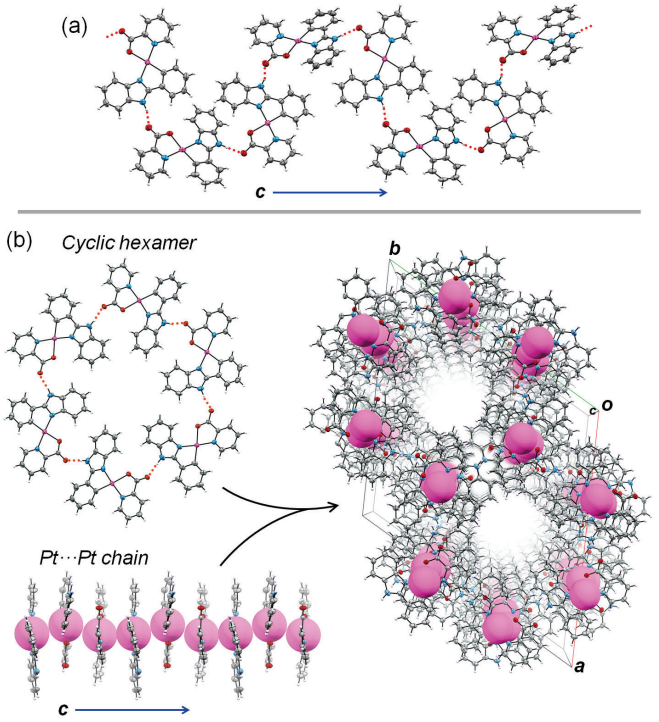

Fig. 1 Packing structures of (a) **1N** and (b) **1P**. Thermal ellipsoids are displayed at the 50% probability level. For clarity, Pt atoms in **1P** are shown with a space-filling model, except for the structure of the cyclic hexamer. Hydrogen bonds are drawn with red dotted lines.

In the initial stages of this study, we attempted various typical crystallisation methods (Table S1) and obtained yellow crystals of **1N** as the major product and orange crystals of **1P** as the minor product. As shown in Fig 1, single-crystal X-ray diffraction (SXRD) analysis revealed that **1N** (Monoclinic $P2_1/c$) and **1P** (Trigonal R) are pseudo-polymorphs of **1**. Although the coordination geometries and hydrogen-bond distances are almost identical for **1N** and **1P** (Fig. S1, Table S2), the packing structures are completely different. **1N** adopted a nonporous packing structure (Fig. S2(a)) composed of a hydrogen-bonded zig-zag chain built from **1** (Fig 1(a)). In this crystal, the shortest Pt···Pt distance (3.8282(3) Å; Fig. S2(b)) is significantly longer than twice the van der Waals radius of Pt (3.5 Å), indicating negligible Pt···Pt interactions in **1N** in the ground state. The powder X-ray diffraction (PXRD) pattern of the as-synthesised form of **1** (blue line in Fig. 2(a)) is identical to the PXRD pattern simulated for the crystal structure of **1N**, suggesting the thermodynamic stability of **1N**. Conversely, hydrogen bonds were used to construct the supramolecular cyclic hexamer of **1** in crystal **1P** (Fig 1(b)), and this hexamer was aligned in the *ab* plane to form a honeycomb-like sheet (Fig. S3(a)). Furthermore, each hexamer was stacked in a helical manner with a 3-fold screw axis (Fig. S3(b,c)), resulting in the formation of a one-dimensional hydrophobic channel with a pore diameter of 7.3 Å (Table S2) and a void fraction of 17%. The Pt···Pt distance (3.5130(4) Å) in **1P** was comparable to twice the van der Waals radius of Pt, revealing the presence of Pt···Pt interactions along the *c* axis. Therefore, **1P** was found to be a PMC constructed of hydrogen bonds and Pt···Pt interactions (Fig 1(b)). However, despite a number of attempts (Table S1), the selective crystallisation of **1P** proved difficult with typical methods (Fig. S4). Although the hydrophobic pore of **1P** was assumed to be stabilised by nonpolar solvents, they were immiscible with good

solvents for **1,** so nonpolar solvents could not be used with the typical methods.

In contrast to these methods, **1P** was selectively crystallised by the dispersion of cyclohexane in a MeOH/H_2O (v/v = 1/1) mixture containing **1** (0.125 mM) and a surfactant (see Experimental section in ESI for details). The SXRD analysis revealed that this resulted in a 1:3 ratio of cyclohexane and **1** molecules in the pores of **1P** prepared by this method (Fig. S5). The inclusion of cyclohexane was also confirmed by the ^{1}H NMR spectrum (Fig. S6(a)) and the thermogravimetric analysis (Fig. S6(b)). The PXRD pattern of the orange polycrystalline powder of **1P** prepared by this method (red line in Fig. 2(a)) is identical to the simulated PXRD pattern based on the crystal structure of **1P**, and the absence of peaks derived from **1N** indicates the high purity of **1P**. Even after desorption of cyclohexane by heating at 155 °C, the packing structure of **1P** was maintained (i.e. permanent porosity[1f]; Fig. S6(c)). In addition, **1P** was obtained regardless of surfactant, suggesting the limited importance of the surfactant (Fig. S7). Conversely, when crystals of **1P** were immersed in the MeOH/H_2O (v/v = 1/1) solution of **1** (0.25 mM) in the absence of a liquid-liquid interface, **1P** dissolved, and crystals of **1N** were deposited instead (Entry 2 in Table S3). Therefore, the cyclohexane serves as a template and stabilises **1P**,[10,11] despite the fact that cyclohexane is immiscible with the MeOH/H_2O mixture. Since a cyclohexane-containing MeOH/H_2O solution of **1** did not afford **1P** (Entry 3 in Table S3) even at 4 °C, the liquid-liquid interface is considered important in obtaining **1P** in this system.

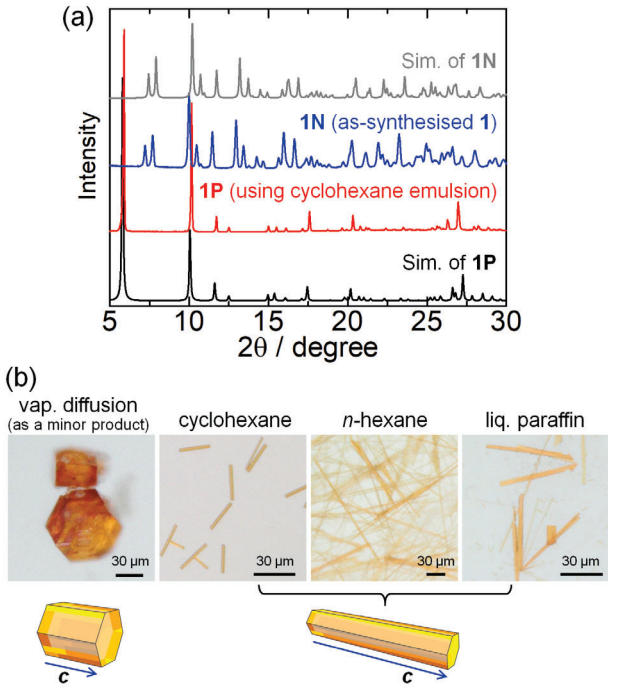

Fig. 2 (a) PXRD patterns of as-synthesised **1** (blue line) and **1P** prepared using cyclohexane emulsion (red line). The black and grey lines indicate the simulated patterns based on the crystal structures of **1P** and **1N**, respectively. (b) Photographs and schematic images of **1P** crystals obtained by vapour diffusion or using emulsions of cyclohexane, *n*-hexane, and liquid paraffin. Arrows indicate the direction of the *c* axis.

To further investigate the crystallisation, several control experiments were carried out. First, emulsions of several linear alkanes (*n*-hexane, *n*-octane, *n*-tetradecane, and liquid paraffin) were employed in place of the cyclohexane emulsion. The desired **1P** was successfully obtained with the use of linear alkanes (Fig. 2(b); Table S4), but the selectivity was lower for *n*-hexane, *n*-octane, and *n*-tetradecane (Fig. S8 and Table S5); therefore, the high **1P**-selectivity for the cyclohexane emulsion likely results from the appropriate size of cyclohexane (~6.0 Å) for the pore diameter of **1P** (7.0-7.3 Å; Table S2), as well as the appropriate 3-fold symmetry of cyclohexane (D_{3d}) relative to that of **1P** (Trigonal *R*). Importantly, the shape of the crystals of **1P** was largely dependent on the crystallisation method, because the crystals obtained using the emulsions of alkanes were needle-like and the crystals obtained using the typical method were block-like (Figs. 2(b) and S8). Since the long axis of the needle-like crystals of **1P** was assignable to the *c* axis (Fig. S7(b)), the use of alkanes would promote crystal growth along the channel direction (i.e. *c* axis). This result is consistent with the fact that the longest **1P** crystals were obtained in the absence of surfactant (Fig. S7(c)), in which case cyclohexane molecules should directly contact the **1P** solution. Thus, as suggested above, the inclusion of alkanes should stabilise the porous channels composed of the supramolecular cyclic hexamer and promote the selective growth of **1P** along the *c* axis in the presence of the liquid-liquid interface.

To observe the crystallisation process directly, optical microscopic observations were conducted (Figs. 3 and S9). For this purpose, a solution of **1** (0.125 mM) in a MeOH/H_2O (v/v = 1/1) mixture was slowly layered onto liquid paraffin to form a flat MeOH/H_2O-liquid paraffin interface. After the layering, micrometre-sized particles appeared at the liquid-liquid interface within several minutes (Figs. 3(a) and S9(a)). These microparticles were characterised as **1P** by synchrotron PXRD analysis (Fig. S9(b)). Conversely, relatively large crystals floated in the solution after 10 min (Fig. 3(b)). Similarly, when using the cyclohexane emulsion, only tiny crystals of **1P** were obtained just after the preparation (Fig. S10), while large crystals of **1P**

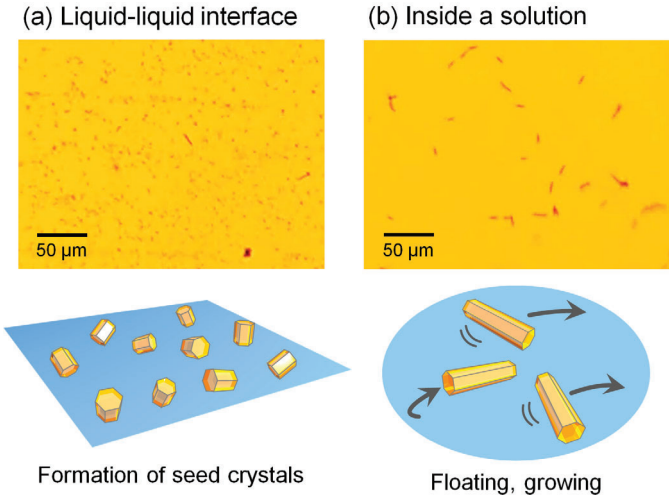

Fig. 3 Optical microscopic images of (a) the interface between a solution of **1** in MeOH/H_2O (v/v = 1/1) mixture and liquid paraffin and (b) the solution of **1**. Images were taken 10 min after layering of a solution of **1** onto liquid paraffin.

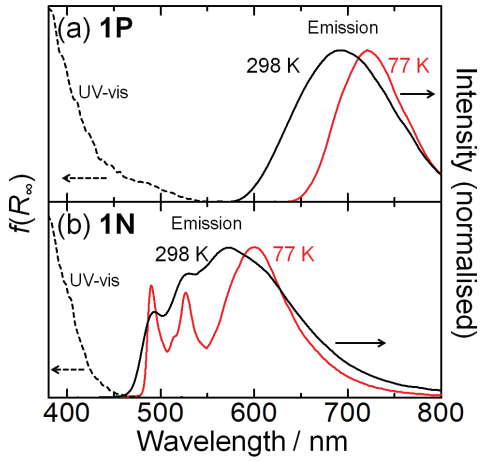

Fig. 4 UV-vis diffuse-reflectance (dashed lines) and emission (solid lines) spectra of (a) **1P** (λ_{ex} = 500 nm) and (b) **1N** (λ_{ex} = 400 nm) in the solid state at 298 K (black) and 77 K (red).

were grown after 1 day. These results indicate the occurrence of the Ostwald ripening in the solution after the formation of seed crystals of alkane-incorporated **1P** at the liquid-liquid interface, and contrast with the fact that a **1P** crystal itself did not serve as a seed crystal in the absence of cyclohexane (Entry 2 in Table S3).

Owing to the different packing structures, **1P** and **1N** exhibited completely different photophysical properties. The UV-vis diffuse-reflectance spectrum of **1P** crystals showed a broad absorption band at 450-550 nm (Fig. 4(a), dashed line), which is absent in **1N** crystals (Fig. 4(b)) and the solution of **1** (Fig. S11). This new absorption band of **1P** is assignable to the singlet metal-metal-to-ligand charge transfer (^{1}MMLCT) transition arising from the Pt···Pt interaction, as supported by the theoretical calculations (Fig. S12). As expected, **1P** displayed red emission (λ_{max} = 692 nm; Fig. 4(a)) from the ^{3}MMLCT excited state, whereas **1N** exhibited yellow emission consisting of several peaks (λ_{max} = 493, 530, and 573 nm; Fig. 4(b)). For **1P**, the broad structureless emission band exhibited a significant red-shift at 77 K (λ_{max} = 721 nm; Figs. 4 and S13(a)), as is typically observed for ^{3}MMLCT emission because of the shortening of Pt···Pt distances at 77 K.[7b,12] In addition, the emission band for **1P** was maintained even after the removal of cyclohexane (Fig. S13(b)), consistent with the permanent porosity of **1P**. Furthermore, the microspectroscopic analysis revealed that the emission bands and the emission lifetimes were identical for several single crystals of **1P** (Figs. S14-S15), revealing the high uniformity of **1P** crystals obtained with this crystallisation procedure. In the case of **1N**, the emission intensities of higher-energy peaks were increased by cooling to 77 K (Fig. 4(b)). Since this higher-energy band is similar to the emission band of **1** in a MeOH/EtOH glass (Fig. S16) and to those of previously reported Pt(II) complexes bearing *N*-substituted pbim,[13] this band is assigned as a ligand-centred $^3\pi\pi^*$ emission band originating from discrete molecules without any Pt···Pt interactions. Additionally, the excitation spectra and the wavelength-dependent emission lifetime measurements suggested that the lower-energy band of **1N** could be assigned as an excimer-like emission (Fig. S17). Overall, the formation of crystal pseudo-polymorphs of **1** at the liquid-liquid interface enabled control of not only the porosity but also the emission properties between ^{3}MMLCT and $^3\pi\pi^*$+excimeric dual emissions.

In conclusion, we have successfully obtained luminescent PMC **1P** at the liquid-liquid interface, and this PMC is not obtained selectively with typical crystallisation methods. This success results from the stabilisation of the pores of the seed crystals by the inclusion of an alkane at the liquid-liquid interface. Consistent with the differences in packing structures, porous **1P** and nonporous **1N** displayed distinctly different photophysical behaviours. The present results indicate that the immiscible solvents promote the crystallisation of PMCs at the liquid-liquid interface, and this constitutes a new strategy for obtaining PMCs effectively.

This work was partly supported by JSPS KAKENHI grant numbers JP17H06367, JP18K19086, and JP18K14232, and also the Iketani Science and Technology Foundation. The PXRD measurements were performed under the approval of the Photon Factory Programme Advisory Committee (Proposal No. 2017G528). The supercomputing resources at the Institute for the Molecular Science in Japan are also acknowledged.

Conflicts of interest

There are no conflicts to declare.

Notes and references

1 For reviews: (a) M. W. Hosseini, *Acc. Chem. Res.*, 2015, **38**, 313; (b) M. I. Hashim, C.-W. Hsu, H. T. M. Le and O. Š. Miljanić, *Synlett*, 2016, **27**, 1907; (c) T. Adachi and M. D. Ward, *Acc. Chem. Res.*, 2016, **49**, 2669; (d) Y.-F. Han, Y.-X. Yuan and H.-B. Wang, *Molecules*, 2017, **22**, 266; (e) I. Hisaki, C. Xin, K. Takahashi and T. Nakamura, *Angew. Chem. Int. Ed.*, 2019, **58**, 11160; (f) R.-B. Lin, Y. He, P. Li, H. Wang, W. Zhou and B. Chen, *Chem. Soc. Rev.*, 2019, **48**, 1362.

2 For reviews: (a) S. Kitagawa, R. Kitaura and S. Noro, *Angew. Chem. Int. Ed.*, 2004, **43**, 2334; (b) O. M. Yaghi, M. O'Keeffe, N. W. Ockwig, H. K. Chae, M. Eddaoudi and J. Kim, *Nature*, 2003, **423**, 705.

3 For reviews: (a) X. Feng, X. Ding and D. Jiang, *Chem. Soc. Rev.*, 2012, **41**, 6010; (b) P. J. Waller, F. Gándara, O. M. Yaghi, *Acc. Chem. Res.*, 2015, **48**, 3053.

4 For recent examples: (a) P. Sozzani, S. Bracco, A. Comotti, L. Ferretti and R. Simonutti, *Angew. Chem. Int. Ed.*, 2005, **44**, 1816; (b) P. Dechambenoit, S. Ferlay, N. Kyritsakas and M. W. Hosseini, *J. Am. Chem. Soc.*, 2008, **130**, 17106; (c) Y. He, S. Xiang and B. Chen, *J. Am. Chem. Soc.*, 2011, **133**, 14570; (d) M. Mastalerz and I. M. Oppel, *Angew. Chem. Int. Ed.*, 2012, **51**, 5252; (e) K. Raatikainen and K. Rissanen, *Chem. Sci.*, 2012, **3**, 1235; (f) A. Karmakar, R. Illathvalappil, B. Anothumakkool, A. Sen, P. Samanta, A. V. Desai, S. Kurungot and S. K. Ghosh, *Angew. Chem. Int. Ed.*, 2016, **55**, 10667; (g) F. Hu, C. Liu, M. Wu, J. Pang, F. Jiang, D. Yuan and M. Hong, *Angew. Chem. Int. Ed.*, 2017, **56**, 2101.

5 (a) C. H. Hendon, K. E. Wittering, T.-H. Chen, W. Kaveevivitchai, I. Popov, K. T. Butler, C. C. Wilson, D. L. Cruickshank, O. Š. Miljanić and A. Walsh, *Nano Lett.*, 2015, **15**, 2149; (b) T. Ogoshi, Y. Shimada, Y. Sakata, S. Akine and T. Yamagishi; *J. Am. Chem. Soc.*, 2017, **139**, 5664; (c) I. Hisaki, Y. Suzuki, E. Gomez, Q. Ji, N. Tohnai, T. Nakamura and A. Douhal, *J. Am. Chem. Soc.*, 2019, **141**, 2111.

6 (a) J. T. A. Jones, D. Holden, T. Mitra, T. Hasell, D. J. Adams, K. E. Jelfs, A. Trewin, D. J. Willock, G. M. Day, J. Bacsa, A. Steiner and A. I. Cooper, *Angew. Chem. Int. Ed.*, 2011, **50**, 749; (b) H. Yamagishi, H. Sato, A. Hori, Y. Sato, R. Matsuda, K. Kato and T. Aida, *Science*, 2018, **361**, 1242.

7 (a) M. Kato, S. Kishi, Y. Wakamatsu, Y. Sugi, Y. Osamura, T. Koshiyama, M. Hasegawa, *Chem. Lett.*, 2005, **34**, 1368; (b) Y. Shigeta, A. Kobayashi, T. Ohba, M. Yoshida, T. Matsumoto, H.-C. Chang and M. Kato, *Chem. Eur. J.*, 2016, **22**, 2682; (c) Y. Shigeta, A. Kobayashi, M. Yoshida and M. Kato, *Cryst. Growth Des.*, 2018, **18**, 3419.

8 For recent examples: (a) S. Takamizawa, T. Akatsuka, U. Ueda, *Angew. Chem. Int. Ed.*, 2008, **47**, 1689; (b) S. Tashiro, R. Kubota and M. Shionoya, *J. Am. Chem. Soc.*, 2012, **134**, 2461; (c) I. Bassanetti, A. Comotti, P. Sozzani, S. Bracco, G. Calestani, F. Mezzadri and L. Marchio, *J. Am. Chem. Soc.*, 2014, **136**, 14883; (d) M. Tadokoro, Y. Ohata, Y. Shimazaki, S. Ishimaru, T. Yamada, Y. Nagao, T. Sugaya, K. Isoda, Y. Suzuki, H. Kitagawa and H. Matsui, *Chem. Eur. J.*, 2014, **20**, 13698; (e) H. Sasaki, H. Imoto, T. Kitao, T. Uemura, T. Yumura and K. Naka, *Chem. Commun.*, 2019, **55**, 6487; (f) S. Chand, S. C. Pal, A. Pal, Y. Ye, Q. Lin, Z. Zhang, S. Xiang and M. C. Das, *Chem. Eur. J.*, 2019, **25**, 1691; (g) T. Seki, K. Ida, H. Sato, S. Aono, S. Sakaki and H. Ito, *Chem. Eur. J.*, 2020, **26**, 735; (h) M. Nakaya. W. Kosaka, H. Miyasaka, Y. Komatsumaru, S. Kawaguchi, K. Sugimoto, Y. Zhang, M, Nakamura, L. F. Lindoy and S. Hayami, *Angew. Chem. Int. Ed.*, 2020, **59**, in press. DOI: 10.1002/anie.202003811.

9 M. Kato, H. Ito, M. Hasegawa and K. Ishii, *Chem. Eur. J.*, 2019, **25**, 5105.

10 (a) F. H. Herbstein, M. Kapon and G. M. Reisner, *J. Incl. Phenom.*, 1987, **5**, 211; (b) I. Hisaki, S. Nakagawa, N. Tohnai and M. Miyata, *Angew. Chem. Int. Ed.*, 2015, **54**, 3008; (c) H. Wang, Z. Bao,H. Wu, R.-B. Lin, W. Zhou, T.-L. Hu, B. Li, J. C.-G. Zhao and B. Chen, *Chem. Commun.*, 2017, **53**, 11150.

11 D. Tanaka and S. Kitagawa, *Chem. Mater.*, 2008, **20**, 922.

12 (a) W. B. Connick, L. M. Henling, R. E. Marsh and H. B. Gray, *Inorg. Chem.*, 1996, **35**, 6261; (b) M. Kato, C. Kosuge, K. Morii, J. S. Ahn, H. Kitagawa, T. Mitani, M. Matsushita, T. Kato, S. Yano and M. Kimura, *Inorg. Chem.*, 1999, **38**, 1638; (c) M. Nakagaki, S. Aono, M. Kato and S. Sakaki, *J. Phys. Chem. C*, 2020, **124**, 10453.

13 (a) H. Li, J. Ding, Z. Xie, Y. Cheng and L. Wang, *J. Organomet. Chem.*, 2009, **694**, 2777; (b) H. Li, J. Li, J. Ding, W. Yuan, Z. Zhang, L. Zou, X. Wang, H. Zhan, Z. Xie, Y. Cheng and L. Wang, *Inorg. Chem.*, 2014, **53**, 810; (c) P.-H. Lanoë, A. Moreno-Betancourt, L. Wilson, C. Philouze, C. Monnereau, H. Jamet, D. Jouvenot, F. Loiseau, *Dyes and Pigments*, 2019, **162**, 967.

Table of Contents

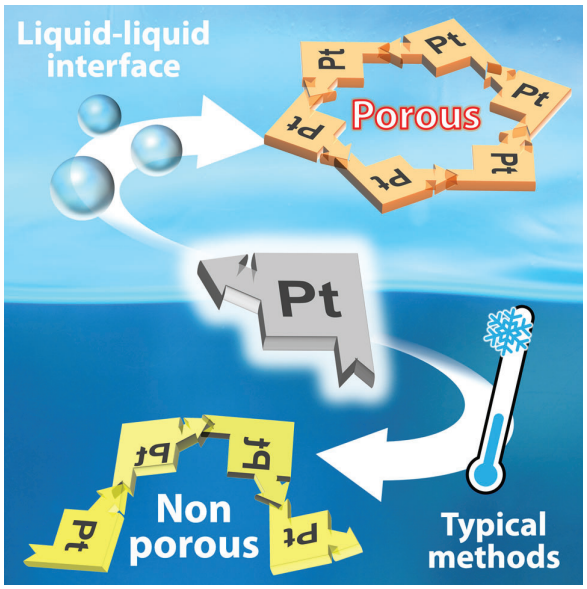

A Pt(II)-based luminescent porous molecular crystal was selectively crystallised at the liquid-liquid interface, allowing the control of porosity and luminescence.